

Spectral Effects on Fast Wave Core Heating and Current Drive

C. K. Phillips 1), R. E. Bell 1), L. A. Berry 2), P. T. Bonoli 3), R. W. Harvey 4),
J. C. Hosea 1), E. F. Jaeger 2), B. P. LeBlanc 1), P. M. Ryan 2), G. Taylor 1), E. J. Valeo 1),
J. R. Wilson 1), J. C. Wright 3), H. Yuh 5), and the NSTX Team

1) PPPL, Princeton University, Princeton, NJ 08540, USA

2) ORNL, Oak Ridge, TN 37831, USA

3) PSFC, MIT, Cambridge, MA 02139, USA

4) CompX, Del Mar, CA 92014, USA

5) Nova Photonics, Princeton, NJ 08540, USA

email contact of main author: ckphillips@pppl.gov

Abstract. RF heating and current drive is an essential component in most magnetic fusion devices, including ITER. Recent results obtained with high harmonic fast wave (HHFW) heating and current drive (CD) on NSTX strongly support the hypothesis that the onset of perpendicular fast wave propagation right at or very near the launcher is a primary cause for reduced core heating efficiency at long wavelengths that is also observed in ICRF heating experiments in numerous tokamaks. A dramatic increase in core heating efficiency was achieved in NSTX L-mode helium majority plasmas when the onset for perpendicular wave propagation was moved away from the antenna and nearby vessel structures. This was accomplished by reducing the edge density in front of the launcher with lithium conditioning and avoiding operational points prone to instabilities, resulting in efficient core heating in deuterium L mode and H mode discharges. These results indicate that careful tailoring of the edge density profiles in ITER should be considered to limit RF power losses to the antenna and plasma facing materials. Finally, in plasmas with reduced rf power losses in the edge regions, the first direct measurements of high harmonic fast wave current drive were obtained with the motional Stark effect (MSE) diagnostic. The location and radial dependence of HHFW CD measured by MSE are in reasonable agreement with predictions from both full wave and ray tracing simulations.

1. Introduction

Radio frequency (rf) heating and current drive (CD) are essential components in many magnetic fusion devices. Experimental and theoretical studies on NSTX are focused on optimizing core heating and current drive efficiency by minimizing power losses in the edge

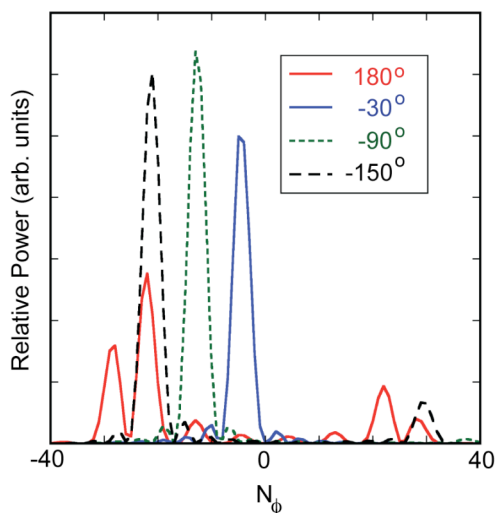


FIG. 1. NSTX antenna spectrum (power coupled into plasma) vs N_ϕ for different phasings

regions, an issue of importance in ITER [1]. These studies are also needed to establish the viability of devices based on the spherical torus (ST) concept, such as ST-CTF [2], which may depend on rf waves to sustain long-pulse reactor-grade plasmas and assist with non-inductive plasma start-up. In the NSTX device, the effectiveness of high harmonic fast waves (HHFW) for providing core heating and $q(0)$ control to establish fully noninductively sustained H-mode scenarios, and for providing HHFW-driven bootstrap current for non-inductive current drive during the ramp-up phase of the discharge, is under investigation.

The HHFW system on NSTX is particularly well suited for studying the competition between core heating and edge power losses as a function of antenna phasing. The NSTX HHFW launcher has

12 antenna straps that can deliver up to 6 MW at 30 MHz [3]. By feeding this strap array with six decoupled sources, very good toroidal spectral definition is obtained. Fig.1 shows the relative power coupled into the plasma as a function of the toroidal mode number, N_ϕ , for various set strap-to-strap phasings, ranging from -30° to $+180^\circ$, calculated with the RANT3D code for plasma conditions typical of those discussed in this paper [3].

Because of the inherently high beta of NSTX plasmas, the HHFWs experience strong nearly single pass absorption via electron Landau damping and transit time magnetic pumping [4]. Shown in Figure 2 are ray paths in the toroidal (a,c) and poloidal (b,d) cross sections, respectively, obtained with the GENRAY code [5] for waves launched with parallel wave numbers, k_{\parallel} , over the range accessible with the 12-strap antenna for typical OH target conditions [$n_{e0} = 3.3 \times 10^{19} \text{ m}^{-3}$, $T_{e0} = 1.1 \text{ keV}$] in (a) and (b), and for the rf-heated plasma conditions [slightly hollow density profile, with $n_{e0} = 2.3 \times 10^{19} \text{ m}^{-3}$, peak $n_e = 2.7 \times 10^{19}$ at $\rho \sim 0.3$, $T_{e0} = 2.8 \text{ keV}$] in (c) and (d). The solid dot at the end of each ray path represents the point at which at least 80% of the power launched on that ray has been absorbed. As expected from theory [6], the absorption rate increases as the plasma is heated and is lower for the ray launched with -30° phasing. However, it is interesting to note that even this ray is strongly absorbed in less than a

single toroidal or poloidal transit of the rf-heated plasmas. The interaction of these waves with the inner wall of the vessel is also minimal, due to the $n_{\parallel}^2 = R$ cutoff [6] that moves significantly into the plasma on the high field side of the magnetic axis. These absorption properties of the HHFWs in NSTX provide the opportunity to study core heating as a function of antenna phasing and to separate out rf power losses near the antenna from rf power losses elsewhere in the plasma.

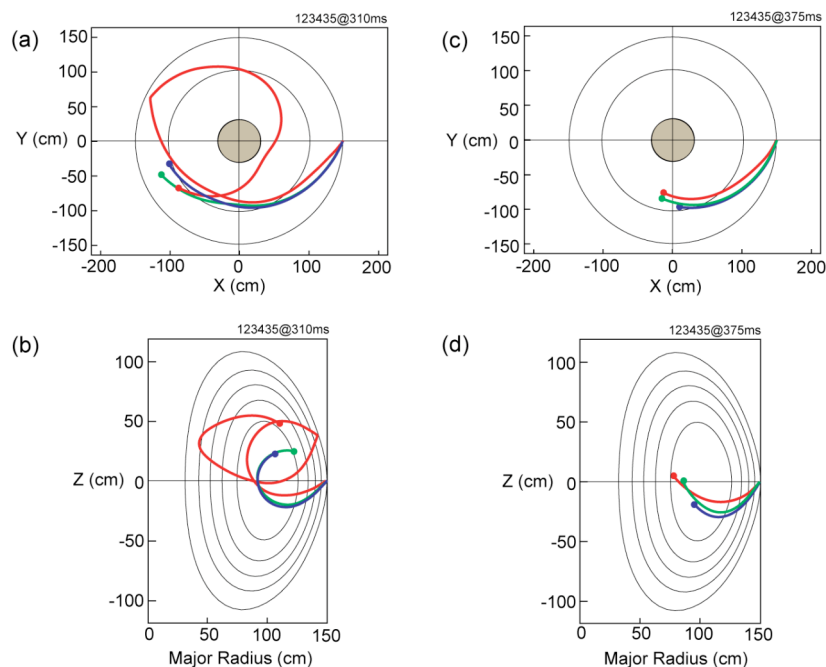


FIG. 2. Ray paths for -30° (red), -90° (blue) and 180° (green) strap-to-strap antenna phasings for OH target conditions (a =toroidal, b=poloidal views) and for rf-heated plasma conditions (c=toroidal, d=poloidal views), for a discharge with $B_{T0} = 0.55 \text{ T}$ and $I_p = 600 \text{ kA}$. Solid dot shows where 80% of initial power is absorbed.

In this paper, experimental studies on NSTX of the dependence of the core heating and current drive efficiency as a function of the antenna phasing are discussed and compared to simulations obtained with a range of advanced state-of-the-art rf simulations. The results of these studies strongly support the hypothesis that the onset of fast wave propagation right at or very near the launcher is a primary cause for the reduced core heating efficiency observed at long wavelengths [7] in NSTX and in ICRF heating experiments in numerous tokamaks. A dramatic increase in core heating efficiency was achieved in NSTX L-mode helium-4 majority plasmas when the edge density was lowered, thereby moving the location where the HHFWs start to propagate away from the antenna and nearby vessel structures. These results

indicate that careful tailoring of the edge density profiles in ITER should be considered to limit rf power losses to the antenna and plasma facing materials. Finally, the location and radial profile of HHFW CD measured with the motional Stark effect (MSE) diagnostic [8], obtained in plasmas with reduced rf power losses in the edge, are in reasonable agreement with simulations obtained from the GENRAY ray tracing code, as well as the AORSA [9] and TORIC [10] full wave codes.

2. Fast Wave Core Heating Efficiencies in NSTX

The core heating efficiency in NSTX in L-mode plasmas composed primarily of helium-4 has been inferred from a series of similar discharges at fixed phasing but different magnetic field strengths, and at fixed magnetic field with a range of phasings. In order to quantify the amount of rf power deposited to the electrons in the core of the plasma, rf power pulses are applied and the time evolution of the electron stored energy, W_e , is fitted with an exponential rise function of the form:

$$W_e(t) = W_0 - (W_0 - W_F) \times (1 - e^{-t/\tau_e}) \quad , \quad (1)$$

where W_0 is the electron stored energy at the beginning of the pulse and W_F is the asymptotic value that would have been obtained in the steady-state limit [7]. The electron stored energy is evaluated by integrating the kinetic electron pressure measured by Thomson scattering over the magnetic field surface volumes inferred from the magnetic equilibrium code, EFIT [11]. The rf-induced change in the electron stored energy, ΔW_e , is equal to the difference between W_F and the asymptotic value of W_e that would have been obtained without the rf pulse, while the rf power into electrons in the core is given by $P_{rf,e} = \Delta W_e / \tau_e$. Finally, the core electron heating efficiency is then defined by $\eta_e = P_{rf,e} / \Delta P_{rf}$, where ΔP_{rf} is the increment in the applied rf power in the pulse. The total core heating efficiency, η_T , is similarly inferred using the time evolution of total stored energy, W_T , obtained from EFIT.

In previous experiments [7] at a fixed toroidal magnetic field of 0.45 T, the core electron heating efficiency for a fixed strap-to-strap phasing of -90° ($k_{//} = -8 \text{ m}^{-1}$) was approximately equal to 22%, or about half of the 48% efficiency achieved with 180° phasing ($k_{//} = 14 \text{ m}^{-1}$). Power losses due to parametric decay instabilities (PDI) and associated edge ion heating were

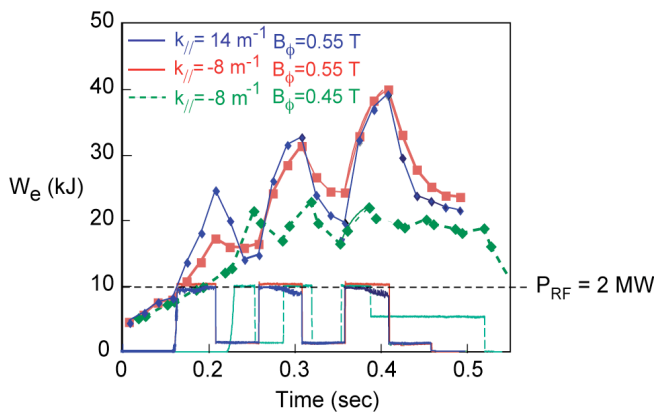


FIG. 3. Time evolution of the electron stored energy during rf heating at different B_T for fixed phasing, and for different phasing at fixed B_T .

comparable for both of these phasings, and hence could not account for the large difference in core heating efficiencies [7]. These experiments were repeated at a higher magnetic field of 0.55 T and results are shown in Fig. 3 and in Fig. 5 later on. As shown in Fig. 3, the change in ΔW_e is about a factor of 2 higher at $B_\phi = 0.55 \text{ T}$ than at 0.45 T for -90° phasing ($k_{//} = -8 \text{ m}^{-1}$). Note however that with the magnetic field fixed at 0.55 T, comparable increments in ΔW_e were obtained at both -90° and 180° phasings for the second and third rf pulses in the discharges, but not in the first pulse where the observed increase in ΔW_e is noticeably less with the -90° phasing ($k_{//} = -8 \text{ m}^{-1}$). During this first rf pulse, the edge density 2 cm in front of the antenna exceeded the critical density for onset of wave propagation perpendicular to the magnetic field at $k_{//} = -8 \text{ m}^{-1}$, but

not during the second and third pulses, when the heating efficiency for both the $k_{\parallel} = -8 \text{ m}^{-1}$ and 14 m^{-1} cases is comparable. Since the critical density needed for wave propagation scales as $B \times k_{\parallel}^2 / \omega$ [6], these results strongly suggest that fast wave propagation near the antenna or vessel wall is a primary cause for the reduced heating efficiency at longer wavelengths.

The propagation of HHFWs can be reasonably simulated using a cold plasma model [4]. In Fig. 4a, the cold plasma wave propagation characteristics for the HHFWs are displayed as a function of the edge density for a magnetic field strength of 0.282 T in front of the antenna, corresponding to the 0.45 T on axis case shown in Fig. 3. For a given k_{\parallel} , if the edge density is too low, the wave is “cut off” ($k_{\perp} = 0$) and does not propagate into the plasma. In this case, the wave will “evanesce” into the plasma until it reaches a point where the local density exceeds the “critical density” and propagation commences. The local group velocity then specifies the direction in which the wave energy subsequently propagates in to the plasma. In Fig. 4b, the angle that the group velocity makes with respect to the edge magnetic field is drawn for

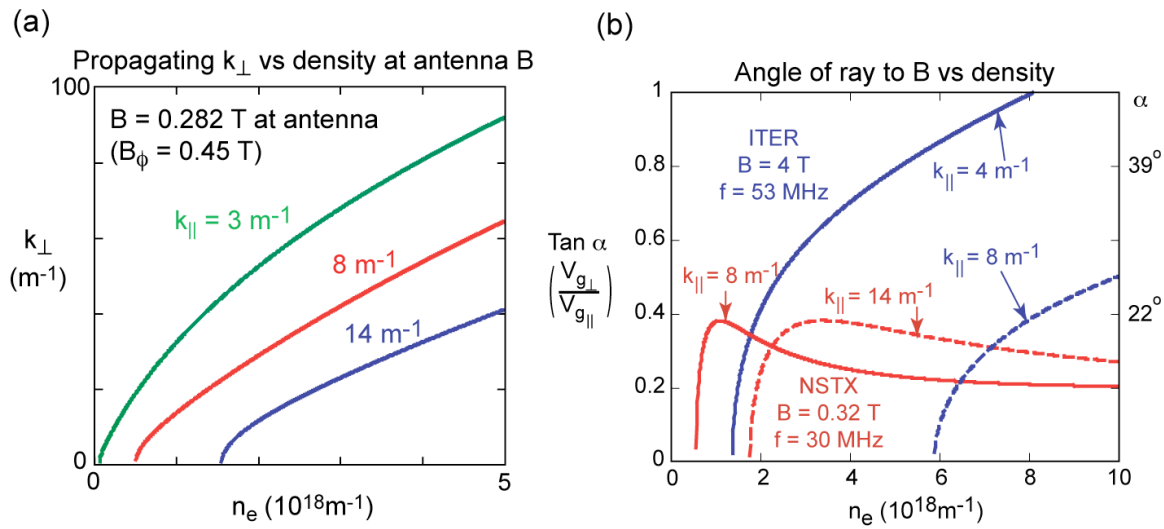


FIG. 4. Dispersion relation (a) and angle of group velocity (b) with respect to magnetic field show that lower phasings propagate closer to the wall for a given density profile.

HHFW heating (180°) and current drive phasings (90°) in NSTX as well as for low harmonic ICRF heating and current drive in ITER. The HHFWs in NSTX tend to propagate at a small angle relative to the equilibrium magnetic field over the range of operating densities, while the lower harmonic fast waves in ITER can penetrate more readily across the field lines as the density encountered by the waves increases.

As inferred from Fig. 4a, for a given edge density profile and magnetic field, the waves with the lower launched k_{\parallel} 's begin to propagate much closer to the antenna than those with higher k_{\parallel} 's. Increasing the edge magnetic field moves the onset for propagation away from the antenna for all values of k_{\parallel} , for a fixed frequency. If the waves begin to propagate too close to the antenna, the NSTX results presented here suggest that power is lost in the edge regions, most likely due to such processes as collisions, rf sheaths, and sputtering associated with direct fast wave interactions in the vicinity of the antenna and surrounding structures. These edge power losses can account for the observed degradation of core heating efficiency at the smaller launched k_{\parallel} . Note however, that previous studies of ICRF heating at lower harmonics indicate that if the distance between the antenna and the point at which propagation begins is too large, that it becomes difficult to couple sufficient power into the plasma. For this reason,

the ITER project is considering enhancing the scrape-off density to improve coupling with a large antenna-plasma gap [1,12]. Since the density profile in the scrape-off region is presumed to be rather flat, it is possible that wave propagation will occur near the blanket surface and the antenna in ITER should the density be increased to or above the critical density for propagation. The NSTX results indicate that careful tailoring of the edge density profiles in ITER should be considered to limit edge power losses from direct fast wave damping.

Previous HHFW heating experiments on NSTX in deuterium plasmas at 0.45 T were rather unsuccessful [7], in part because control of the density is more difficult in deuterium than in helium operation, so the edge densities tended to be higher. After extensive wall conditioning and avoidance of MHD activity, HHFW heating in deuterium plasmas at the higher magnetic field of 0.55 T was as successful as that in helium plasmas [3], as seen in Fig. 5. Indeed, central electron temperatures of 5 keV have now been achieved in both He and D plasmas at $B_T = 0.55$ T with the application of 3.1 MW HHFW at -150° antenna phasing [13]. The rf

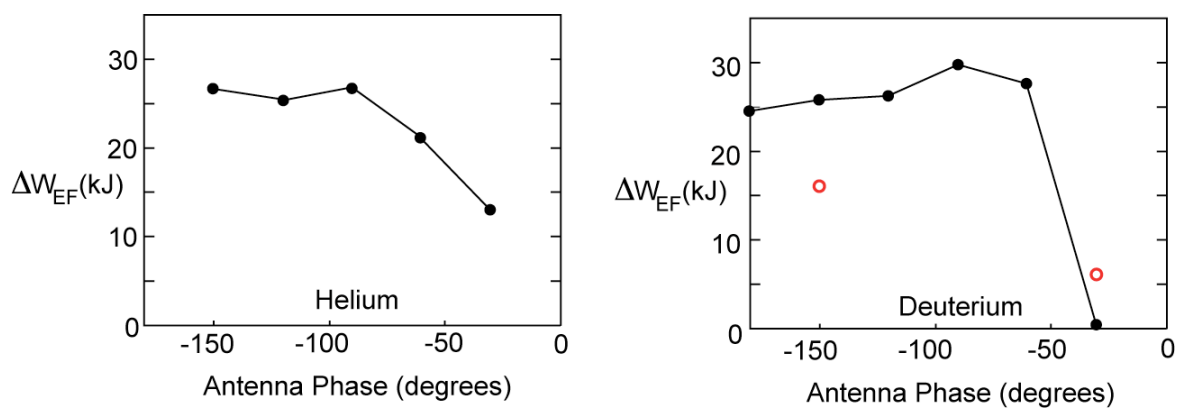


FIG. 5. RF-induced increments in electron stored energy comparable in both He-4 ($P_{rf} \sim 1.8$ MW) and D ($P_{rf} \sim 1.1$ MW) discharges. Red circles indicate results obtained with shorter rf pulses ($P_{rf} \sim 1.3$ MW) in discharges with Li plasma conditioning.

induced change in electron stored energy still dropped precipitously below -60° phasing for this initial phase scan in deuterium. According to the Thomson scattering diagnostic, the edge density for the -30° discharge was significantly higher than in the other discharges in the scan, most likely due to an MHD instability whose presence correlated with the time evolution of the edge density. Analysis indicates the edge density was above the critical density for propagation, consistent with the conclusion that high edge densities lead to increased edge power losses and corresponding degradation of the core heating efficiency. With additional edge conditioning obtained with lithium injection, a further reduction in the edge density at -30° phasing was observed with the edge reflectometer [14], resulting in the first significant heating in D plasmas at this phasing, as indicated by the open red circle at -30° in Fig. 5. However, the rf pulse length in the discharges with Li conditioning were only about 67 msec in duration, compared to the 230 msec duration for the scan of deuterium discharges shown in Fig. 5. As a result, the stored energy increment obtained at -150° phasing in the discharges with the Li conditioning was less than in the longer discharges without it. Because of this difference in rf pulse lengths, it is difficult to accurately compare the performance of the discharges. Nevertheless, these studies indicate that extensive conditioning to reduce the edge density results in better core heating efficiencies over a range of antenna phasings, consistent with the conclusion that edge power losses can be significant if the wave begin to propagate too close to the launcher and surrounding structures.

3. MSE Measurements of HHFW Current Drive

By operating at higher magnetic fields and with reduced edge densities, the first direct measurements of HHFW co-current drive [7] at an antenna phasing of -90° were obtained with the motional Stark effect (MSE) diagnostic [8]. The MSE measurements, obtained using modest rf power (~ 1.8 MW) and short rf pulses (~ 80 msec), indicate that about 15 kA of noninductive current was driven by the HHFWs within $\rho \leq 0.2$, as shown in Fig. 6. The

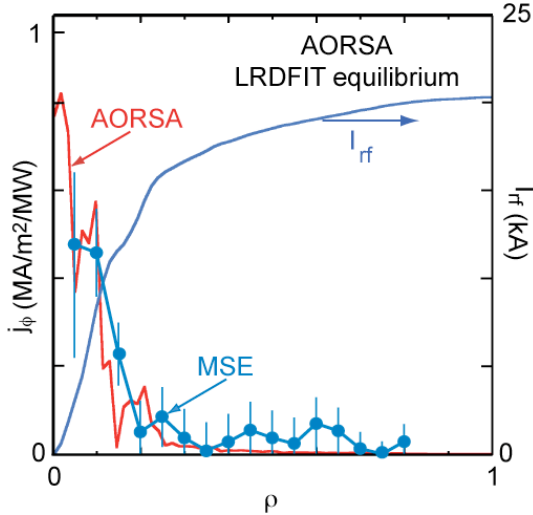


FIG. 6. Comparison of MSE data with AORSA full spectrum simulation using LRDFIT

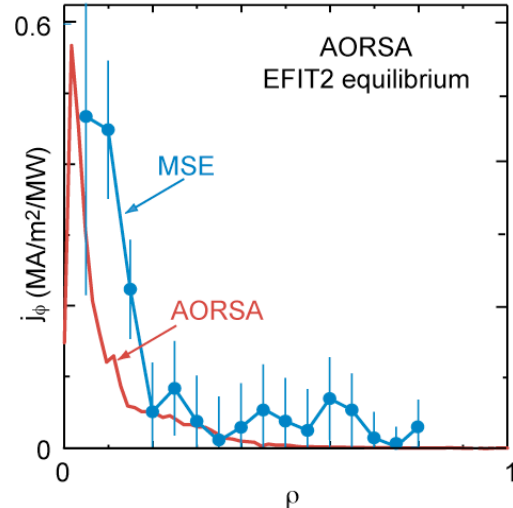


FIG. 7. Comparison of MSE data with AORSA full spectrum simulation using EFIT2

magnitude of the driven current profile is normalized assuming that 67% of the launched power, or about 1.2 MW of power, is actually coupled into the core plasma, consistent with changes in the stored energy of the discharge. The simulations obtained with the AORSA code [9], using the Ehst-Karney (E-K) parameterization [15] and the full spectrum of launched waves, are shown in Fig. 6 for comparison. Electron trapping effects effectively limit the rf-driven current to the plasma core in NSTX and other ST devices, consistent with the MSE data and previous modeling studies [16]. It is important to note that agreement between the simulations and the measurements improves as the plasma parameters used in the simulations are more tightly constrained by experimental measurements. In particular, better agreement is found by using an equilibrium fit from the LRDFIT code [17] that is constrained by the actual MSE pitch angle measurements and kinetic plasma profiles as shown in Fig. 6, rather than the less constrained equilibrium from EFIT2 as shown in Fig. 7.

Simulations of the noninductive driven current in this discharge obtained with the AORSA and TORIC full wave codes, using the E-K parameterization, are remarkably consistent, as shown in Fig. 8. The noninductive driven current density profiles are shown for the single peak toroidal mode number, $N_\phi=12$, launched by the HHFW antenna. Note that the predicted magnitude of the noninductive currents is considerably higher than that obtained with the full spectrum, shown in

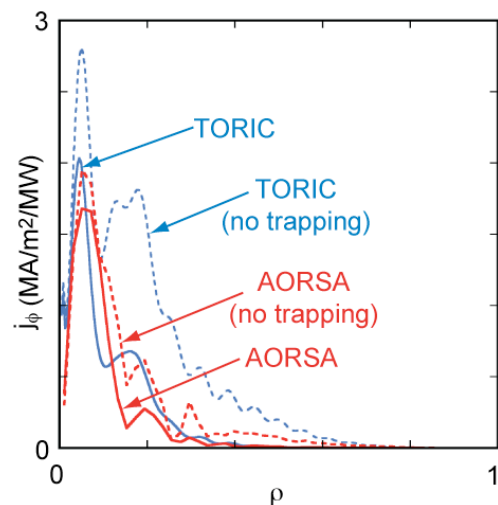


FIG. 8. AORSA and TORIC simulations, with and without trapping, for $N_\phi=12$.

Fig. 6, indicating the importance of including the back lobes of the spectrum in the simulations. The simulations indicate that power on the back lobe, launched at a very high k_{\parallel} , is damped well off-axis where the corresponding noninductive driven current is lost due to trapping effects. This effectively reduces the power available for current drive by about 50%, thereby accounting for the difference in magnitude between the integrated currents found with the full spectrum in Fig. 6 and the single N_{ϕ} spectrum in Fig. 8. The E-K parameterization is based on solutions of the adjoint equation for rf-driven currents in conventional aspect ratio tokamaks. Simulations with the GENRAY code, which can solve for the induced current using the ADJ module [18] that solves the adjoint equation for the exact NSTX equilibrium are underway and will be compared in the future to the MSE data and the full-wave simulations provided here. As these wave modules are integrated into the TRANSP transport analysis code [19], further simulation studies will be able to examine the impact of neglecting the back EMF on the driven current profile (the assumption of steady-state conditions).

4. Conclusions

The results obtained with HHFW heating and CD on NSTX strongly support the hypothesis that the onset of fast wave propagation right at or very near the launcher is a primary cause for the reduced core heating efficiency observed at long wavelengths [7] in ICRF heating experiments in numerous tokamaks. Since the critical density needed for wave propagation scales as $B \times k_{\parallel}^2 / \omega$ [6], moving the location at which the fast waves begin to propagate away from the antenna and nearby structures, by increasing the magnetic field and extensive conditioning to reduce the edge density, resulted in better core heating efficiencies over a range of antenna phasings. The observed degradation at the lowest antenna phasing is thus most likely due to power losses from collisions, rf sheaths, and sputtering associated with direct fast wave interactions in the vicinity of the antenna and surrounding structures. The effect is particularly pronounced in NSTX since the HHFWs are nearly totally damped in a single transit of the device. It is thus likely that the main power losses to the edge occur from the initial interactions with the antenna and surrounding structures. This makes the NSTX plasma an ideal test-bed for benchmarking models in advanced RF codes for RF power loss in the vicinity of the antenna. Numerical studies to evaluate the relative importance of these various edge loss mechanisms are underway in the RF SciDAC project [20]. The ITER project is considering enhancing the scrape-off density to improve coupling with a large antenna-plasma gap [1,12]. The NSTX results indicate that careful tailoring of the edge density profiles in ITER should be considered to limit edge power losses from direct fast wave interactions with the antenna and plasma facing materials.

Experiments have begun on NSTX to optimize HHFW core heating of neutral beam driven H-mode deuterium plasmas. Again with a well conditioned wall, significant core electron heating, as evidenced by an increase ~ 0.7 keV in $T_e(0)$ and a factor of ~ 2 in central electron pressure has been observed for 0.55 T operation with an antenna phase of 180° ($k_{\phi} = \pm 14 \text{ m}^{-1}$, 18 m^{-1}) [13]. This result contrasts strongly with the total lack of heating found earlier at $B_T = 0.45$ T, and is useful for the study of electron transport in the NSTX core plasma [21]. Over the next few years, NSTX experiments will explore HHFW CD in L- and H-mode deuterium plasmas with longer rf pulses and higher rf power to permit more accurate and nearer steady state MSE measurements. Simulations obtained thus far with the AORSA and TORIC full wave codes, using the E-K parameterization, are remarkably consistent with MSE measurements of approximately 15 kA of noninductive driven current within $\rho \leq 0.2$ for 1.8 MW of input rf power (~ 1.2 MW absorbed). The comparisons highlight the impact of trapping effects on noninductive currents driven off-axis and indicate the need to optimize the

launched spectrum to minimize trapping-related degradation in the current drive efficiency. However, even with the modest power and rf pulse lengths used so far, the rf-driven current is sufficient to transiently decrease $q(0)$ from 1.0 to 0.6, as inferred from the pitch angles near the axis measured by the MSE diagnostic. With the ability to drive both co and counter CD, the HHFW system may therefore provide a tool for $q(0)$ control, needed to achieve long pulse high performance discharges in NSTX and future ST and other fusion devices.

Work supported by USDOE Contract No. DE-AC02-76CH03073.

- [1] Swain, D. W., and Goulding, R. H., *Fusion Eng. Des.* **82** (2007) 603.
- [2] Peng, Y-K. M., et al., *PPCF* **47** B263 (2005).
- [3] Ryan, P. M., et al., *35th EPS Conference on Plasma Physics* paper P1.108 (June 2008, Hersonissos, Crete, Greece).
- [4] Ono, M., *Phys. Plasmas* **2** (1995) 4075.
- [5] Smirnov, A. P., and Harvey, R. W., *Bull. Am. Phys. Soc.* **48** (1995) 1837; also Report CompX-2000-01, Ver.2 March 17, 2003.
- [6] Stix, T. H., *Waves in Plasmas*, [AIP, NY, 1992].
- [7] Hosea, J., et al., *Phys. Plasmas* **15**, 056104 (2008).
- [8] Levinton, F. M., et al., *Phys. Plasmas* **14**, 056119 (2007).
- [9] Jaeger, E. F., et al., *Phys. Plasmas* **8**, 1573 (2001).
- [10] Brambilla, M., *Plasma Phys. and Controlled Fusion* **44**, 2423 (2002).
- [11] Sabbagh, S. A., et al., *Nucl. Fusion* **41** (2001) 1601.
- [12] Nightingale, M., personal communication, 2007.
- [13] Gates, D., et al., paper OV/3-1 at this conference.
- [14] Wilgen, J. B., et al., *Rev. Sci. Instr.* **77**,1 (2006)1
- [15] Ehst, D. A. and Karney, C. F. F., *Nuclear Fusion* **31** (1991) 1933.
- [16] Mau, T. K., et al., *15th Topical Conference on RF Power in Plasmas*, Moran, Wyoming, 2003, edited by Forest, C. B. (AIP Conference Proceedings, 2005), Vol. 694, p. 205.
- [17] Menard, J., personal communication, 2007.
- [18] Smirnov, A. P., Harvey, R. W., and Prater, R., "General Linear RF-Current Drive Calculations in Toroidal Plasma", Proc. EC-15 Conference, Yosemite, CA, March 2008.
- [19] Hawryluk, R. J., et al., in *Physics of Plasmas Close to Thermonuclear Conditions* (Commission of the European Communities, Brussels, 1980), Vol. 1, pg. 19.
- [20] Bonoli, P. T., et al., *17th Topical Conference on RF Power in Plasmas*, Clearwater, Florida, 2007, edited by Ryan, P. M. and Rasmussen, D. A. (AIP Conference Proceedings, 2005), Vol. 933, p. 435.
- [21] LeBlanc, B.P., et al., *16th Topical Conference on RF Power in Plasmas*, Park City, Utah, 2005, edited by Wukitch, S. J. and Bonoli, P. T. (AIP Conference Proceedings, 2005), Vol. 787, p. 86.